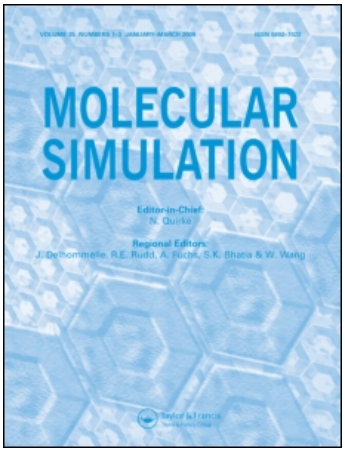

Molecular Simulation

Publication details, including instructions for authors and subscription information:
http://www.informaworld.com/smpp/title~content=t713644482

Catalytic activity of Ti-doped NaH nanoclusters towards hydrogenation of terminal alkenes

S. Chaudhuri[a]; J. T. Muckerman[a]

[a] Chemistry Department and Center for Functional Nanomaterials, Brookhaven National Laboratory, Upton, NY, USA

Online publication date: 27 July 2010

To cite this Article Chaudhuri, S. and Muckerman, J. T.(2007) 'Catalytic activity of Ti-doped NaH nanoclusters towards hydrogenation of terminal alkenes', Molecular Simulation, 33: 11, 919 — 924

To link to this Article: DOI: 10.1080/08927020701502024

URL: http://dx.doi.org/10.1080/08927020701502024

Molecular Simulation, Vol. 33, No. 11, September 2007, 919–924

Taylor & Francis
Taylor & Francis Group

Catalytic activity of Ti-doped NaH nanoclusters towards hydrogenation of terminal alkenes

S. CHAUDHURI†* and J. T. MUCKERMAN

Chemistry Department and Center for Functional Nanomaterials, Brookhaven National Laboratory, Upton, NY 11973-5000, USA

(Received January 2007; in final form June 2007)

The reported activity of nanoscale NaH and titanocene towards catalytic reduction of terminal alkenes using molecular hydrogen is surprising considering that both NaH bulk and titanocene are inactive by themselves. In this work, the role of Ti dopants, the importance of NaH nanoclusters and role of the solvent (THF) and cocatalyst (titanocene) are investigated using density functional theory techniques. A plausible mechanism is proposed to explain the origin of the selective catalytic activity. A step-by-step reaction pathway starting with hydrogen chemisorption near the titanium atoms on the NaH nanoparticle surface followed by the reaction of the activated hydrogen with terminal alkenes via a five-membered ring intermediate are discussed.

Keywords: DFT; Nanoscale; Catalysis; First-principles; Alkene

1. Introduction

Alkali metal hydrides are well known as hydriding agents. Effective alkali and alkaline earth metal hydrides towards hydrogenation reactions are limited to LiH, NaH, MgH_2, BeH_2 and their complex metal hydrides and borohydrides ($LiAlH_4$, $NaAlH_4$, $LiBH_4$, $NaBH_4$, $Mg(BH_4)_2$, etc.). Another traditional class of catalysts used for the selective hydrogenation of olefins includes transition metals such as Ni, Pt, Pd, Rh, etc. [1–6]. The activity of transition metal catalysts in *syn*-hydrogenation inversely follows the trend of the activation barrier for the chemisorption of molecular hydrogen. The use of alkali metal hydrides in commercial systems is limited because of their lack of long-term stability despite their cost effectiveness, and in some cases their pyrophoric nature.

Hydrides, borohydrides and complex metal hydrides such as MgH_2, $LiBH_4$, $NaAlH_4$, etc. are also important as promising hydrogen storage materials. They are the lightweight (thus higher hydrogen content by weight) and low-cost alternative to transition metals and metal alloys mentioned above in the context of ease of hydrogen chemisorption. However, their effectiveness in emulating the activity of transition metals is critically linked to the catalytic chemisorption of molecular hydrogen. This is due to the need to regenerate the hydride under near-ambient operating conditions to achieve reversibility. It is not surprising that transition metal dopants in dilute amounts can lower the relatively high barrier for hydrogen chemisorption [7]. It is clear that finding candidate catalysts for chemisorption of molecular hydrogen to form hydrides has strong links to our understanding of the role of similar transition metal catalysts relevant in heterogeneous catalytic reactions. The latter area has been extensively studied by organic and polymer chemists for decades. First principles calculations have also contributed significantly to a systematic understanding of complex catalytic processes including different transition metal surfaces, metallocenes and other Ziegler–Natta-derived metal complexes [8,9]. The mechanistic studies often involve hydrogen chemisorption at the catalytically active sites on the surface followed by various reaction pathways possible for the activated hydrogen depending on the subsequent reactant and required reaction conditions. The similarity of these reactions prompted us to look in more detail into one of the systems that we found to be suitable for hydrogen chemisorption: a NaH surface doped with titanium. We found that this

*Corresponding author. Email: chaudhuri@wsu.edu
†Current address: Applied Sciences Laboratory, Washington State University, Spokane, WA 99210, USA.

Molecular Simulation
ISSN 0892-7022 print/ISSN 1029-0435 online © 2007 Taylor & Francis
http://www.tandf.co.uk/journals
DOI: 10.1080/08927020701502024

surface chemisorbs hydrogen and the activated hydrogen can promote a reaction of NaH nanoparticles and bis(cyclopentadienyl) titanium dichloride (Cp_2TiCl_2) towards the selective hydrogenation of terminal alkenes [10–12]. We have investigated this reaction with the hope of providing a link between the mechanism discussed in this work and the general principle of hydrogenation catalysts discussed above. The possible role of titanocene that we infer from our preliminary studies is limited to providing NaH-supported Ti-centers, i.e. the active sites. This is consistent with the experimental report that finds no evidence of catalytic activity from the solution phase that contains titanocene although it is known to be active in other homogeneous catalytic reactions [13].

1.1 NaH doped with titanium as catalyst

Before we proceed to discuss the results of our first principles calculations, it will be useful to discuss the reaction under consideration in more detail. Firstly, the selective hydrogenation of terminal alkenes is performed under THF with NaH and titanocene (Cp_2TiCl_2) acting as cocatalysts. There is no known catalytic activity of bulk NaH under similar reaction conditions. The reason for the catalytic activity of nanoparticulate NaH proposed in the literature points to the high surface area of nanoscale NaH used (particle size around 2–30 nm and BET surface area 90 m^2) [11]. Secondly, the NaH phase is prepared from a mix of naphthalene, metallic Na and $TiCl_4$ under a flow of hydrogen gas. This can also produce nanoparticles with some titanium already present in dilute amounts. The high reactivity is attributed to Cp_2TiCl_2 supported on the reductive medium, the nanometric NaH particle, although no difference in reactivity with varying concentrations of titanocene is seen [11]. The slight differences in reactivity shown by the substituted titanocene derivatives do not follow any conclusive trend to support direct participation of titanocene molecules. Finally, the heterogeneous phase, i.e. the solid phase consisting of NaH with adsorbed titanium atoms, when tested separately showed initial catalytic activity but the solution phase showed no such activity. The reactivity of this catalyst is much higher than the conventional catalysts and as a result, it can be a cost effective alternative to the Pt-, Pd- or Ni-based hydrogenation catalysts. The main problem that proved to be detrimental to the prospects of this catalyst is the slow but steady degradation of the initial burst of catalytic activity. Here, we will present evidence to support our suggested catalytic mechanism and identify probable side reactions on the NaH surface that might be responsible for the catalyst degradation.

2. Methods

We have used Kohn–Sham density functional theory (DFT) [14,15] to calculate the ground-state properties of the reactants, surfaces and the transition states of the intermediates. We have used the generalized gradient approximation (GGA) to include a better description of the inhomogeneities in charge densities, a situation relevant for the calculations of reactivity, activation barriers and bond rearrangements. The GGA changes the expression for the exchange-correlation functional by adding the gradient of spin densities ($\nabla n_\downarrow + \nabla n_\uparrow$) whereas only local spin densities ($n_\downarrow + n_\uparrow$) are used in the local density approximation (LDA). The generalized form of the exchange-correlation (XC) functional in the GGA is:

$$E_{\mathrm{XC}}^{\mathrm{GGA}}(n_\uparrow, n_\downarrow) = \int d^3 r f(n_\uparrow, n_\downarrow, \nabla n_\downarrow + \nabla n_\downarrow) \qquad (1)$$

For periodic calculations, faster performance is possible by using plane waves to describe the *lattice periodic part* in the reciprocal lattice space. The electronic wave-function represented by using a plane wave basis set thus only requires the sum of plane waves along the reciprocal lattice vectors, **G**:

$$\psi_{j,\mathbf{k}}(\mathbf{r}) = \sum_{\mathbf{G}} c_{j,\mathbf{k}}\mathbf{G} e^{i(\mathbf{G}+\mathbf{k})\cdot\mathbf{r}} \qquad (2)$$

Ultrasoft plane wave pseudopotentials as implemented in the program CASTEP were used in this work to describe the core electrons in the periodic DFT calculation [16]. The ultrasoft pseudopotentials use fewer plane waves to generate smoother pseudo-wave-functions when the norm conservation constraint is removed by means of partitioning the total electron density in hard and soft components [17]. We have used the Revised Perdew–Burke–Ernzerhof (RPBE) exchange and correlation functional (E_{XC}) for its reliability in predicting accurate chemisorption energies [18–23]. Convergence with respect to the plane wave basis set cut-off value and Monkhrost–Pack k-mesh densities was tested. The calculations presented here have a cut-off of 370 eV and k-mesh density of $8 \times 8 \times 2$. For the calculations involving non-periodic systems (e.g. the NaH nanocluster), all-electron atomic orbital basis sets called DNP (double ζ numeric basis sets with polarization functions for main group elements including hydrogen) were used. This technique, as implemented in the program DMOL3 is suitable for examining the orbital interactions in the reaction between the olefin and surface sites [24]. Chemisorption followed by reaction with propene was investigated in vacuum and in THF using the COSMO solvent model [25,26]. For modeling solvent interactions, VWN–BP exchange and correlation functionals were used for all the calculations on the reaction between the nanocluster and the olefin. LST–QST (linear synchronous transit/quadratic synchronous transit) transition state searches were carried out to find the transition state and potential energy barrier for the reaction in vacuum and in solution [27].

2.1 Modeling reactants and products

We have chosen the NaH (001) surface, the most stable surface of the binary hydride NaH with rocksalt structure, to study the reactivity and probable reaction pathways. The NaH unit cell and atomic positions were first optimized using the quasi-Newtonian Broyden–Fletcher–Goldfarb–Shanno (BFGS) algorithm starting with the crystallographic data. Unit cell parameters from the optimized structure are within 1% of the published crystallographic structure. We then cleaved a 2 × 2 periodic surface in the (001) direction from the optimized unit cell. Three atomic layers at the bottom were kept fixed to represent the bulk followed by two more atomic layers for representing the surface. The vertical periodic image of this surface was separated by a large layer of vacuum (30 Å) above the surface atomic layer. The resultant periodic unit was relaxed to attain a total energy minimum. For subsequent calculations, the bottom three layers were kept fixed. This periodic surface was optimized again when the surface was doped with a single Ti^+ ion replacing a Na^+. The replacement with a cation of the same charge is important for maintaining overall charge neutrality and obtaining the correct ground state energy. This model surface was then tested for its reactivity towards molecular hydrogen.

The cluster calculations were performed on a 1 nm cubic cluster carved from the bulk rocksalt NaH lattice containing a total of 100 atoms. The optimization of this cluster produces a NaH cluster with rounded corners and edges, a morphology expected due to the radially outward Coulombic forces. Then one Na^+ ion was replaced by a Ti^+ on one of the (001) faces. This model was explored for reactivity in a manner similar to the periodic surface calculations described above. The following reaction was studied:

$$H_2 + H_2C{=}CH{-}CH_3 \xrightarrow[\text{THF}]{np-\text{NaH}+\text{TiCp}_2\text{Cl}_2} CH_3CH_2CH_3 \quad (3)$$

The alkene chain length was kept to a minimum to isolate the effect of the hydrogenation catalyst on the energetics of the reaction. Using this model, it is possible to introduce further complexity and try to understand the effect of chain length, different electron withdrawing and electron donating substituents, etc. The reaction pathway and transition state calculations involved all 636 electrons associated with the 111 atoms with 1091 valence orbitals and were optimized for a total of 333 degrees of freedom (111 × 3).

3. Results and discussion

The rationale behind the Ti-containing active site was based on our ongoing study of hydrogen chemisorption catalysts in transition metal doped metal hydrides. We found that among the alkali metal hydrides, NaH doped with a very dilute amount of titanium can promote the exothermic chemisorption of hydrogen and form a TiH_2 species on the surface. The effectiveness of Ti-doped NaH as a chemisorption catalyst is low because the hydrogen atoms are strongly bound to the Ti with no low-temperature diffusion path for forming dissociated hydride species. The alkene reaction studied here stood out as a candidate for the removal and propagation of the hydrogenation reaction cycle. We will discuss two distinct steps of this process: (1) hydrogen chemisorption on a NaH nanocluster doped with Ti^+ (figure 1) and (2) the reaction of the activated hydrogen with the terminal alkene.

3.1 Step 1: hydrogen chemisorption

A NaH(001) surface doped with Ti(+1) chemisorbs hydrogen molecules. This chemisorption process is a result of the overlap between the H_2 anti-bonding orbital and the surface LUMO near Ti atoms where the out-of-plane $3d_{xz}$-type orbital provides the suitable symmetry for donation of electron density from the surface HOMO to the stabilized combination of $\sigma^*_{H_2}$– surface LUMO. The net result is populating the hydrogen anti-bonding orbital which causes an exothermic dissociation of the H—H bond driven by the formation of Ti—H bonds (MO diagram shown in figure 2). We could not identify any significant barrier for this reaction, so we consider the first stage of the reaction to be spontaneous chemisorption within the errors involved in calculating barriers in a GGA–DFT calculation.

The overall hydrogen chemisorption reaction is exothermic by 0.94 eV (21.6 kcal/mol) per H_2 in the flat periodic surface. The same reaction is exothermic by 1.06 eV (24.5 kcal/mol) per H_2 in the nanocluster. The hydrogen chemisorption process is possible on a flat periodic doped NaH surface and on the surface of a doped nanocluster. The probability of a Ti atom being accommodated in a sodium site is higher for a surface with defects, and small nanoparticles are most probably a convenient way of creating such sites.

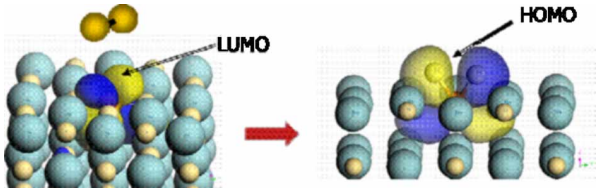

Figure 1. Surface frontier molecular orbitals associated with the formation of the titanium-hydrogen chemisorbed species: (a) the surface LUMO before chemisorption and (b) the surface HOMO after the formation of an adduct by overlap with the H_2 σ^* orbital.

3.2 Step 2: hydrogenation of terminal alkene

The initial chemisorption reaction produces a TiH_2 species with two activated hydrogen atoms, as show in figure 1. The catalytic activity of the Ti center on the NaH nanocluster or surface will depend on how efficiently these hydrogen atoms can be utilized in the next step. A *syn*-hydrogenation of the olefin in a manner analogous to Pt, Pd, Ni, etc. can produce an alkane. This will also free up the Ti center for further participation in the catalytic cycle.

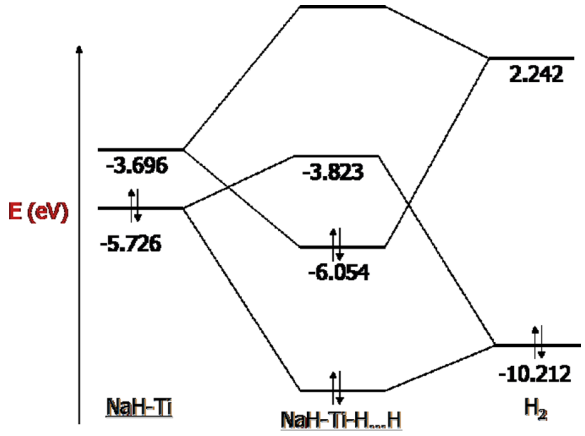

Figure 2. A partial MO diagram showing the crossover of the unreacted surface LUMO and the surface HOMO when the LUMO and the σ* molecular orbital from the hydrogen molecule form a stabilized combination.

We have used the simplest terminal alkene, propene ($CH_3CH{=}CH_2$) to search for the possible existence of such a reaction mechanism. Propene is used in these preliminary calculations to separate the electronic structure effects of this reaction from steric effects and substitution effects. The hydrogen absorption step was spontaneous in the gas phase but the second step is an activated process. We found that the gas phase barrier for this reaction from a LST/QST search is as high as 0.38 eV (8.8 kcal/mol). The hydrogenation reaction of propene is exothermic by 0.52 eV (12 kcal/mol). We have examined the transition state (saddle point) structure to understand the reaction mechanism. The transition state can be described as a distorted five-membered ring consisting of the two carbon atoms from the alkene, the two hydrogen atoms and the titanium atom at the active site (shown in figure 3). The five-membered ring is distorted with a short and a long C—H bond. The Ti has a Mulliken charge of +0.299 indicating partial reduction in the positive charge (the Ti charge was +0.407 before reaction).

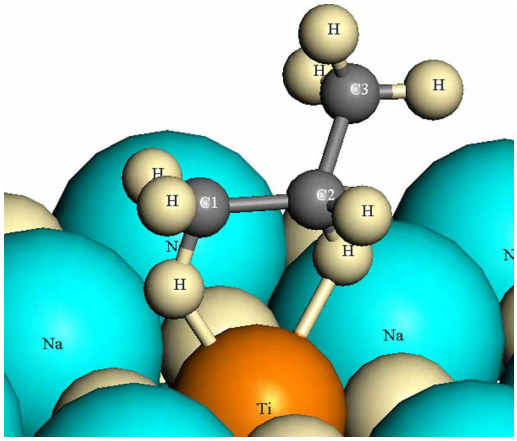

Figure 3. The gas-phase transition state is shown. It contains a five-membered ring and the C2—H bond is shorter than the C1—H bond.

The partial Mulliken charges of the carbon atoms are C1 = −0.261, C2 = −0.261, C3 = −0.268. The trend shows that C3, which is already sp3 hybridized, is the most negative carbon atom. Carbon atoms C1 and C2 have the same Mulliken charge. The C1—H* bond (where the "*" is used to indicate activated hydrogen atoms) is slightly longer than the C2—H* bond (1.135 vs. 1.108 Å) and the H—C1—C2 bond angle is 110.08°). The other two hydrogen atoms at the C1 carbon have an H—C1—H angle of 116.618°. The bond distance between C1 and C2 (1.527 Å) is also slightly shorter than the C2—C3 bond (1.542 Å). All the above suggests that our LST/QST transition state search finds a transition state in which even the terminal carbon is not in a fully hybridized sp^3 state.

We performed spin-unrestricted (spin polarized) SCF calculations using same basis set and found that spin polarization is not preferred. It is not possible to address the question of whether the two Ti—H bonds break in a concerted fashion or sequentially through a singlet biradical intermediate using density functional theory, which is not well suited for including multiconfigurational effects. For example, a transient species with dominant singlet biradical character cannot be expressed as a single-determinant wave-function, and at the very least requires a calculation at the CASSCF(2,2) level. The transition state geometry, however, explains the origin of the selectivity shown by this reaction towards terminal alkenes. The terminal carbon with two hydrogen atoms is nearly planar and parallel to the particle surface in the transition state. This would not be possible if one or both of the hydrogen atoms on the terminal carbon atom are replaced by alkyl groups. Even substitution by a methyl group would increase the reaction barrier significantly and inhibit formation of an alkene adduct before hydrogenation of the terminal double bond. The position of the Ti atom is another important factor that can lower the activation barrier. We are exploring the dependence of the activation barrier on the location of the Ti atom and preliminary results suggest that if we move the optimized transition state complex to one of the edges of the nanocluster and reoptimize the cluster geometry, the transition state energy is lowered by as much as 0.16 eV (3.7 kcal/mol).

3.2.1 Solvent effects. We investigated the role of the solvent in stabilizing H_2 and the nanoparticle. The first step was to explore the possibility of THF blocking the active site. We did not find any significant interaction between THF with the active sites. THF is a polar solvent (dipole moment 1.73 Debye and dielectric constant 7.52) with high miscibility in water. THF is widely used for reactions involving organometallic compounds. Examples of THF use includes Grignard reagents, Ziegler–Natta catalysts, etc. It is believed to have a stabilizing effect through solvation for cations and organometallic adducts. We have used the COSMO and COSMO–RS models [26] to recalculate the energies of reactants, products and the transition states.

Our calculated barrier in THF is 0.18 eV (4.13 kcal/mol). This is less than half the gas-phase reaction barrier (0.38 eV). It is also in agreement with the high initial turnover rates reported for this reaction [11]. The changes in the electronic structure due to solvation effects are also interesting. In the NaH—TiH_2, i.e. hydrogen chemisorbed cluster, the HOMO and LUMO energies are raised by solvent interaction. These orbital energies of the unsolvated cluster shown in figure 2 are −6.054 and −3.823 eV. After solvation by THF, the same molecular orbitals are located at −4.914 and −2.665 eV. The HOMO–LUMO gap (2.231 vs. 2.249 eV) does not change significantly upon solvation. In the transition state the HOMO and the LUMO are located at −3.8 and −3.7 eV compared to −2.341 and −2.196 eV in the solvated state. However, the overall energy of both the reactant and transition state are lowered due to solvation and the net lowering is primarily due to the TS energy being lowered by 3 eV compared to 2.15 eV for the hydrogen chemisorbed NaH—Ti cluster. The charges on carbon atoms are slightly more negative than the gas phase values and are different for all the three carbon atoms in the alkene chain. They are −0.262, −0.274, −0.284 for C1, C2, C3 respectively. The Ti atom charge is relatively unchanged compared to the gas phase (0.297 vs. 0.299).

3.2.2 Side reactions. The initial high rate of activity is very encouraging for practical use of this low-cost catalyst. The prospect that there can be a nanoparticle with gas-phase catalytic activity is another interesting direction to lower the cost of the catalyst. The promise of this system is greatly diminished by the fact that the initial high activity slowly deteriorates and the reaction slows down considerably after two hours. An important criterion for a catalyst to be of industrial grade is lifetime. We have investigated the probable side reactions for this system and found that the most probable one is similar to a Ziegler–Natta type reaction in the solution phase. At any point in time in the THF medium the H_2 molecule, the alkane and the alkene molecules are competing for the bare Ti center. Strong bonding is possible between the Ti atom and the reactant alkene itself. They form a very stable complex via formation of a Ti—C═C η^2 complex (figure 4). The reaction between the bare Ti-doped NaH nanocluster and propene is exothermic by 1.63 eV (37.62 kcal/mol). It has a reaction barrier as high as 0.43 eV (10 kcal/mol), but once formed, it would be hard to dissociate due to the intrinsic thermodynamic barrier. This reaction is in direct competition with a much faster spontaneous hydrogen chemisorption reaction which is also exothermic by 1.06 eV (24.5 kcal/mol). As a result, there is a probable side reaction that will slowly but irreversibly poison the active sites. This is a very common mechanism for catalyst deactivation. As a result, lower temperatures and other ways of running the reaction at lower concentration of alkenes might be useful in prolonging the high activity.

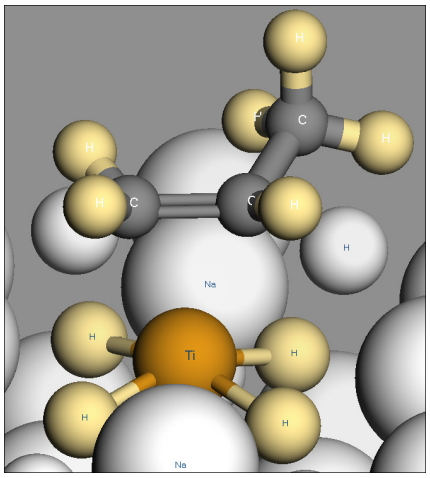

Figure 4. A competitive reaction can be identified for this model nanocluster where a Ti—C═C complex is formed between the titanium atom and the carbon–carbon double bond. Once formed, it will be hard to dissociate the complex under normal reaction conditions.

4. Conclusion

The first principles results presented in this work provide a plausible reaction mechanism that explain the source of the catalytic activity. A Ti atom supported on a NaH nanocluster has been shown to promote spontaneous chemisorption of hydrogen. The chemisorbed hydrogen can take part in selective hydrogenation of terminal alkenes. The mechanism proposed also provides an explanation for the selectivity of this catalyst towards terminal alkenes. The electronic structure of the nanoparticle-alkene transition state and the barrier height were recalculated under THF solvation. Solvation effects alone lower the barrier from 0.38 to 0.18 eV (8.8–4.13 kcal/mol). Our study also provides a probable mechanism by which a catalyst poison, the alkene itself, can lower the catalytic activity of this otherwise highly active catalyst. The simple mechanistic insights discussed here can be useful for the search of improved synthetic routes and ways of improving stability.

Acknowledgements

This work was performed at Brookhaven National Laboratory (BNL) under Contract No. DE-AC02-98CH10886 with the US Department of Energy and supported by it Division of Chemical Sciences, Office of Basic Energy Sciences. Additional support was provided by BNL's Center for Functional Nanomaterials (CFN), a BNL LDRD (No. 05-021) award, and a DOE BES Hydrogen Fuel Initiative award (BO-130). This manuscript has been authored by Brookhaven Science Associates, LLC.

References

[1] M. K. Oudenhuijzen, J. A. van Bokhoven, J. T. Miller, D. E. Ramaker, D. C. Koningsberger. Three-site model for hydrogen adsorption on supported platinum particles: Influence of support ionicity and particle size on the hydrogen coverage. *J. Am. Chem. Soc.*, **127**, 1530 (2005).

[2] V. Pallassana, M. Neurock. Electronic factors governing ethylene hydrogenation and dehydrogenation activity of pseudomorphic Pd-ML/Re(0001), Pd-ML/Ru(0001), Pd(111), and Pd-ML/Au(111) surfaces. *J. Catal.*, **191**, 301 (2000).

[3] V. Pallassana, M. Neurock, L. B. Hansen, J. K. Norskov. First principles analysis of hydrogen chemisorption on Pd-Re alloyed overlayers and alloyed surfaces. *J. Chem. Phys.*, **112**, 5435 (2000).

[4] V. Pallassana, M. Neurock, L. B. Hansen, B. Hammer, J. K. Norskov. Theoretical analysis of hydrogen chemisorption on Pd(111), Re(0001) and Pd-ML/Re(0001), Re-ML/Pd(111) pseudomorphic overlayers. *Phy. Rev. B.*, **60**, 6146 (1999).

[5] S. W. Wang, M. W. Radny, P. V. Smith. Ab initio HF/DFT studies of the chemisorption of hydrogen on the cluster simulated Si(111)-(root 3x root 3)R30 degrees-Al and -Ga surfaces. *Surf. Sci.*, **396**, 40 (1998).

[6] W. Dong, G. Kresse, J. Hafner. Dissociative adsorption of H-2 on the Pd(111) surface. *J. Mol. Catal. A—Chem.*, **119**, 69 (1997).

[7] S. Chaudhuri, J. T. Muckerman. First-principles study of Ti-catalyzed hydrogen chemisorption on an Al surface: a critical first step for reversible hydrogen storage in NaAlH4. *J. Phys. Chem.*, **109**, 6952 (2005).

[8] M. Seth, T. Ziegler. Theoretical study of the copolymerization of ethylene and propylene by a heterogeneous Ziegler-Natta catalyst. *Macromolecules*, **37**, 9191 (2004).

[9] M. Seth, T. Ziegler. Polymerization properties of a heterogeneous Ziegler-Natta catalyst modified by a base: a theoretical study. *Macromolecules*, **36**, 6613 (2003).

[10] Q. Sun, R. A. Sun. Hydrogenation of olefins catalyzed by highly active titanocene/NaH or n-BuLi catalyst systems. *Chem. Res. Chin. Univ.*, **18**, 307 (2002).

[11] Y. H. Fan, S. J. Liao, J. Xu, F. D. Wang, Y. L. Qian, J. L. Huang. Extremely active catalysts for the hydrogenation of terminal alkenes. *J. Catal.*, **205**, 294 (2002).

[12] Y. H. Fan, S. J. Liao, J. Xu, Y. L. Qian, J. L. Huang. Highly active hydrogenation catalysts from titanocenes and sodium hydride of nanometric size. *Chem. J. Chin. Univ.—Chin.*, **18**, 1683 (1997).

[13] N. A. Petasis, Y. H. Hu. Cyclopentadienyl titanium derivatives in organic synthesis. *Curr. Org. Chem.*, **1**, 249 (1997).

[14] W. Kohn, L. Sham. KS equations. *Phys. Rev.*, **140**, 1133 (1965).

[15] R. G. Parr, W. T. Yang. *Density-Functional Theory of Atoms and Molecule*, Oxford University Press, Oxford (1989).

[16] M. D. Segall, P. J. D. Lindan, M. J. Probert, C. J. Pickard, P. J. Hasnip, S. J. Clark, M. C. Payne. First-principles simulation: ideas, illustrations and the CASTEP code. *J. Phys. Condens. Matter.*, **14**, 2717 (2002).

[17] D. Vanderbilt. Soft self-consistent pseudopotentials in a generalized eigenvalue formalism. *Phys. Rev. B*, **41**, 7892 (1990).

[18] J. K. Vincent, R. A. Olsen, G. J. Kroes, M. Luppi, E. J. Baerends. Six-dimensional quantum dynamics of dissociative chemisorption of H-2 on Ru(0001). *J. Chem. Phys.*, **122**, 44701 (2005).

[19] W. P. Krekelberg, J. Greeley, M. Mavrikakis. Atomic and molecular adsorption on Ir(111). *J. Phys. Chem. B*, **108**, 987 (2004).

[20] M. Mavrikakis, J. Rempel, J. Greeley, L. B. Hansen, J. K. Norskov. Atomic and molecular adsorption on Rh(111). *J. Chem. Phys.*, **117**, 6737 (2002).

[21] M. Marlo, V. Milman. Density-functional study of bulk and surface properties of titanium nitride using different exchange-correlation functionals. *Phys. Rev. B*, **62**, 2899 (2000).

[22] B. Hammer. Adsorption, diffusion, and dissociation of NO, N and O on flat and stepped Ru(0001). *Surf. Sci.*, **459**, 323 (2000).

[23] B. Hammer, L. B. Hansen, J. K. Norskov. Improved adsorption energetics within density-functional theory using revised Perdew-Burke-Ernzerhof functionals. *Phys. Rev. B*, **59**, 7413 (1999).

[24] B. Delley. *J. Chem. Phys.*, **113**, 7756 (2000).

[25] A. Klamt, G. Schuurmann. Cosmo - a new approach to dielectric screening in solvents with explicit expressions for the screening energy and its gradient. *J. Chem. Soc. Perkin Trans.*, **2**, 799 (1993).

[26] J. Tomasi, M. Persico. Molecular-interactions in solution - an overview of methods based on continuous distributions of the solvent. *Chem. Rev.*, **94**, 2027 (1994).

[27] T. A. Halgren, W. N. Lipscomb. Synchronous-transit method for determining reaction pathways and locating molecular transition-states. *Chem. Phy. Lett.*, **49**, 225 (1977).